HHS Public Access

Author manuscript

Neuroscience. Author manuscript; available in PMC 2019 September 01.

Published in final edited form as:

Neuroscience. 2018 September 01; 387: 178–190. doi:10.1016/j.neuroscience.2018.01.047.

The changing sensory and sympathetic innervation of the young, adult and aging mouse femur

Stephane R. Chartier[1], **Stefanie A.T. Mitchell**[1], **Lisa A. Majuta**[1], and **Patrick W. Mantyh**[1,2,*]

[1]Department of Pharmacology, University of Arizona, Tucson, AZ 85724

[2]Cancer Center, University of Arizona, Tucson, AZ 85724

Abstract

Although bone is continually being remodeled and ultimately declines with aging, little is known whether similar changes occur in the sensory and sympathetic nerve fibers that innervate bone. Here, immunohistochemistry and confocal microscopy were used to examine changes in the sensory and sympathetic nerve fibers that innervate the young (10 days post-partum), adult (3 months) and aging (24 months) C57Bl/6 mouse femur. In all three ages examined, the periosteum was the most densely innervated bone compartment. With aging, the total number of sensory and sympathetic nerve fibers clearly declines as the cambium layer of the periosteum dramatically thins. Yet even in the aging femur, there remains a dense sensory and sympathetic innervation of the periosteum. In cortical bone, sensory and sympathetic nerve fibers are largely confined to vascularized Haversian canals and while there is no significant decline in the density of sensory fibers, there was a 75% reduction in sympathetic nerve fibers in the aging vs. adult cortical bone. In contrast, in the bone marrow the overall density/unit area of both sensory and sympathetic nerve fibers appeared to remain largely unchanged across the lifespan. The preferential preservation of sensory nerve fibers suggests that even as bone itself undergoes a marked decline with age, the nociceptors that detect injury and signal skeletal pain remain relatively intact.

Keywords

skeletal; nociceptors; pediatric; genetic disorders; geriatric

INTRODUCTION

The study of chronic skeletal pain most commonly focuses on diseases such as osteoarthritis, low back pain and fragility fractures which are due in large part to the age-related decline in the mass, quality and strength of the skeleton (Heaney, Abrams et al. 2000, Melton, Johnell et al. 2004, Mantyh 2014). However, there are over 500 human genetic

*Corresponding Author: pmantyh@email.arizona.edu (PWM).

All other authors report no conflict of interest.

disorders of bone and cartilage. In many cases, the first symptom that prompts diagnosis of these disorders is chronic skeletal pain in the young neonatal and pediatric patient (McCarthy 2011, Boyce 2017). Genetic disorders of bone and joint which are accompanied by significant skeletal pain include; osteogenesis imperfecta (Rauch, Travers et al. 2002, Semler, Netzer et al. 2012, Hoyer-Kuhn, Semler et al. 2014, Ward, Bardai et al. 2016, Boyce 2017), giant cells tumor (Chawla, Henshaw et al. 2013, Karras, Polgreen et al. 2013, Martin-Broto, Cleeland et al. 2014, Gossai, Hilgers et al. 2015), aneurysmal bone cyst (Lange, Stehling et al. 2013, Pelle, Ringler et al. 2014), fibrous dysplasia (Boyce, Chong et al. 2012, Naidu, Malmquist et al. 2014), Paget's disease (Grasemann, Schundeln et al. 2013) and juvenile arthritis (Clinch and Eccleston 2009, Boyce 2017).

Given that much of the young skeleton is cartilaginous and the peripheral nervous system is still developing (Brandi and Collin-Osdoby 2006, Sacchetti, Funari et al. 2007), a major question is where in the young skeleton are the nociceptors that drive this pain and do nerves in the young bone have the same organization, distribution and density as sensory and sympathetic nerve fibers in adult bone? Similarly, an interesting but largely unanswered question is whether as the mass, quality and strength of bone and cartilage decline with age (Exton-Smith, Millard et al. 1969, Woolf and Pfleger 2003), do the nerves that innervate the skeleton also undergo a marked decline?

One issue that has greatly hindered attempts to directly compare the innervation of young, adult and aging skeletons is that whereas young bone generally requires no decalcification prior to tissue sectioning (as it is mostly cartilaginous) both the adult and aging bone are highly calcified and require significant decalcification before tissue sectioning (Hukkanen, Konttinen et al. 1992, Mantyh, Jimenez-Andrade et al. 2010, Jimenez-Andrade and Mantyh 2012, Chartier, Thompson et al. 2014). Previous studies have suggested that many antibodies that work well in the non-calcified tissues frequently showed marked loss of immunostaining when subjected to the decalcification process (Arnold 1988, Shi, Key et al. 1991, Schulze, Witt et al. 1997, Hayat 2002, Mach, Rogers et al. 2002, Mantyh, Jimenez-Andrade et al. 2010, Chartier, Thompson et al. 2014).

To address this problem, in the present study the young mouse femur was used as a positive control, as this skeletal tissue can be processed for immunohistochemistry with or without decalcification and then stained with antibodies raised to a variety of antigens. While many antibodies showed significant loss of signal with decalcification, three antigens that showed virtually no loss of immunostaining between the non-decalcified and decalcified young femur and which worked very well in the young, adult and aging femur were; calcitonin gene related peptide (CGRP) which labels thinly or unmyelinated peptidergic sensory nerve fibers (Kruger, Silverman et al. 1989, Hukkanen, Konttinen et al. 1993, Clinch and Eccleston 2009), tyrosine hydroxylase (TH) which is expressed by postganglionic adrenergic sympathetic nerve fibers (Parfitt 2006, Manolagas and Parfitt 2010), and platelet endothelial cell adhesion molecule (PECAM-1 and also known as CD31) which labels the endothelial cells of blood vessels (Chartier, Thompson et al. 2014).

In light of the above observations, in the present study antibodies to CGRP, TH and CD31, age related changes in sensory nerves, sympathetic nerves and blood vessels were explored

in the mouse femur. The femur was chosen as it is the largest load bearing bone in the body. It clearly shows an age-related decline in mass and strength, and fracture of this bone in humans and mice is accompanied by significant pain (Jimenez-Andrade, Martin et al. 2007, Koewler, Freeman et al. 2007, Freeman, Koewler et al. 2008, Jimenez-Andrade, Bloom et al. 2009, Chartier, Thompson et al. 2014). The mouse was chosen as it is the most commonly used experimental species in modeling human genetic diseases of bone and cartilage (McCarthy 2011) as well as in studies of the injured, diseased and aging skeleton (Mantyh 2014).

EXPERIMENTAL PROCEDURES

Animals

Experiments were performed with young (n=30), adult (n=30) and aging (n=30) male C57Bl/6J mice (Jackson Laboratories, Bar Harbor, ME) that were 10 days post-partem, 3 months and 24 months of age, respectively. For all qualitative assessments, the number of animals was equal to or greater than 10 and for all quantitative data the "n" was ≥ 5. The mice were housed in accordance with the National Institutes of Health guidelines under specific pathogen-free conditions in autoclaved cages maintained at 22°C with a 12-hour alternating light/dark cycle and access to food and water ad libitum. All procedures adhered to the guidelines of the Committee for Research and Ethical Issues of the International Association for the Study of Pain and were approved by the Institutional Animal Care and Use Committee at the University of Arizona (Tucson, AZ, USA)

Preparation of tissue for immunohistochemistry and histology

Tissue from young (10 days) mice and adult (3 months) and aging (24 months) mice were euthanized and processed according to previously published protocols (Thompson, Chartier et al. 2016). Young mice (10 days) were deeply anesthetized with CO2 delivered from a compressed gas cylinder then decapitated. Young hindlimbs were then excised and placed in 4% formaldehyde/12.5% picric acid solution in 0.1 M PBS (pH 6.9 at 4 °C) overnight. Following fixation, young tissue was either placed in PBS (pH 7.4) for 48 hours and then cryoprotected in 30% sucrose at 4°C or the femurs were then placed in decalcified solution for 2 weeks in 0.5M ethylenediaminetetraacetic acid (EDTA) (PBS, pH 8.0 at 4 °C) and then cryoprotected in 30% sucrose at 4°C for at least 48 hours before sectioning. Thus, half of the young femurs were placed in the same decalcification solution as required for the mineralized adult and aging femurs while the other young femurs were cryo-sectioned without going through the decalcification process (i.e. the control limbs). These controls were performed in order to assess the potential effects that the decalcification process had on immunohistochemical staining of a variety of antibodies.

Adult and aging mice (3 and 24 months, respectively) were deeply anesthetized with ketamine/xylazine (0.01 ml/g, 100 mg/10 kg, s.c.) and perfused intracardially as previously described (Chartier, 2014). Similar to young tissue that was placed in the decalcification solution, adult and aging tissue was placed in 4% formaldehyde/12.5% picric acid solution in 0.1 M PBS (pH 6.9 at 4 °C) overnight. Following fixation, the femurs were decalcified for approximately 2 weeks in 0.5M ethylenediaminetetraacetic acid (EDTA) (PBS, pH 8.0 at

4 °C). In all cases, the EDTA solution was changed every day and in the adult and aging animals the decalcification was monitored radiographically with a Faxitron MX-20 digital cabinet X-ray system (Faxitron/Bioptics, Tucson, AZ, USA). Following total decalcification, each femur was cryoprotected in 30% sucrose at 4 °C for at least 48 hours before being sectioned.

Tissue sections of young, adult and aging femurs were cut at either 20 or 60 μm serially and thaw mounted with two sections of bone per gelatin-coated slide. Sections at 20 μm thickness were stained with Safranin O and 60 μm thick sections were used for immunofluorescence staining.

Immunohistochemistry and histology

In the present study, we focused on the distal end of the femur although a similar organization and age-related changes reported here were observed in other parts of the femur. A full protocol of the histology and immunohistochemical techniques used here can be found in a previous publication from our lab (Chartier et al., 2014). Briefly, following sectioning slides were dried at room temperature (RT) for 30 minutes and then washed in PBS for 3 × 10 minutes. Next, the slides were blocked with 3% normal donkey serum (Jackson ImmunoResearch, Cat# 017-11-121; West Grove, PA, USA) in PBS with 0.3% Triton-X 100 (Sigma Chemical Co., Cat# X100; St. Louis, MO, USA) for 1 hour. Afterwards, the slides were incubated overnight with primary antibodies made in 1% normal donkey serum and 0.1% Triton-X 100 in 0.1 M PBS at RT. Peptide-rich sensory nerve fibers were labeled with an antibody against calcitonin gene-related peptide (CGRP; polyclonal rabbit anti-rat CGRP; 1:10,000; Cat #8198; Sigma Chemical Co.). Sympathetic nerve fibers were identified using an antibody against tyrosine hydroxylase (TH; polyclonal rabbit anti-mouse TH, 1:1000, Cat #AB152; Millipore, Temecula, CA, USA). Endothelial cells were labeled using an antibody against cluster of differentiation 31 which is a 140 kD glycoprotein known as platelet endothelial cell adhesion molecule and a member of the immunoglobin superfamily involved in leukocyte transmigration, angiogenesis, and integrin activation (CD31; polyclonal rabbit anti-mouse CD31, 1:500, Cat #550274; BD Pharmingen, San Jose, CA, USA). Nerve growth factor (NGF), a neurotrophic factor that regulates the survival, development, and function of sensory and sympathetic neurons, was labeled using an antibody from Santa Cruz (Dallas, TX, USA), polyclonal rabbit anti-mouse, 1:1000, Cat# SC-548. The preferential membrane receptor for NGF was labeled with an antibody for tropomyosin-related kinase A (TrkA, polyclonal goat anti-mouse, 1:1000, Cat# AF1056; R&D Systems, Minneapolis, MN, USA). The receptor p75 which is low affinity neurotrophin receptor that binds NGF and the other members of the neurotrophin family was labeled with an antibody for p75 (polyclonal rabbit anti-mouse, 1:1000, Cat# AB1554; Millipore, Temecula, CA, USA). Additional antibody information can be found in Table 1.

After primary antibody incubation, preparations were washed 3 × 10 minutes each in PBS and incubated for 3 hours at RT with secondary antibodies conjugated to fluorescent markers (Cy3/Dylight 488/AlexaFluor; 1:600 and 1:400; Jackson ImmunoResearch). Preparations were then washed 3 × 10 minutes each in PBS. Cellular nuclei were labeled using 4′,6-diamidino-2-phenylindole (DAPI) (1:500; Cat#D21490; Invitrogen, Grand Island, NY, USA)

followed by an additional 3 × 10 min wash in PBS. Slides for histological and immunofluorescence were dehydrated through an alcohol gradient (2 minutes each; 70%, 80%, 90%, and 100%), cleared in xylene (2 × 2 minutes), and cover slipped with di-n-butylphthalate-polystyrene-xylene (Sigma Chemical Co., Cat#06522; St. Louis, MO). Preparations were allowed to dry covered at RT for 12 hours before imaging.

Bright field and laser confocal microscopy

Bright field images of histologically stained sections were acquired using an Olympus BX51 microscope fitted with an Olympus DP70 digital CCD. Confocal images of CGRP, TH, CD31, TrkA, p75, NGF and DAPI were acquired using an Olympus FV1200 microscope (Olympus Life Sciences, Center Valley, PA) and a 60x/1.42 PlanApo N objective using excitation beams of 488 and 599 nm, and emissions were detected using BA505-540 and B575-620 emission filters. Nuclear staining (4′,6-diamidino-2-phenylin-dole [DAPI]) was visualized using an excitation beam of 405 nm and emissions were detected using a BA430-470 emission filter. Sequential acquisition mode was used to reduce bleed-through from fluorophores. The average volume of data that was collected was 211.7 μm × 211.7 μm × 60 μm, with each Z-axis slice being 1.0 μm/slice.

Periosteal Thickness

In order to measure the thickness of the fibrous and cambium layers of the periosteum, images (TIFF format) acquired under the DAPI channel were opened in Fiji (Schindelin, Arganda-Carreras et al. 2012). For both the fibrous and cambium layers, three measurements using the “straight” tool, perpendicular to the cortical wall, were taken of the fibrous and cambium layers of the periosteum. The three total measurements were averaged together in Microsoft Excel and data was presented in μm.

Frequency, Innervation and Vascularization of Haversian Canals

In order to measure the occurrence of Haversian canals in young, adult and aging femurs, 60 μm thick sections were used. For each animal analyzed, three 60 μm sections (1 section per slide) were viewed using an Olympus BX51 bright field/fluorescence microscope and an UPlanSApo 10x/0.40 objective. For each section, the cortical bone compartment in the distal end of the femur was analyzed under the DAPI fluorescence filter as this nuclear stain allowed for easy visualization of the unique morphology of a Haversian canal. The total number of Haversian canals, regardless of blood vessel or nerve fiber staining, were then tabulated in Excel. Next, the same section was analyzed again using the corresponding fluorescence filter for CD31 blood vessels, CGRP sensory fibers and then TH sympathetic fibers. The total number of Haversian canals that were CD31+ or CD31-were tabulated and compared with those that were either CGRP+ or TH+ or lacked any nerve fiber staining. All data was entered into Microsoft Excel and the formulas within the program were used to calculated the percentages.

Nerve fiber density

For quantification, frozen sections were used, as cross-sectional analysis allowed for the visualization of the anatomy of the bone and articular cartilage (such as the condyles and

growth plate), which enabled the observer to locate the same anatomical area when quantifying different animals. For each animal analyzed, at least 3 images were obtained for each of the 3 quantified bone compartments: periosteum, bone marrow and cartilage. Images were acquired at least 100 μm apart in the vertical Z plane (i.e. two sections) to minimize duplication of quantifications. Nerve fibers were manually traced using Fiji (an open-source, analytic software program) and added together for a total nerve fiber length (mm). To measure the surface area (mm^2) of each tissue in each region, we analyzed the same tissue sections from which nerve fiber counts were obtained. The nerve fiber density (mm/mm^2) was then divided by the section thickness (0.06 mm) to obtain the volumetric nerve fiber density. The area of bone was measured from the frontal section of the femur and digital images were acquired using an Olympus FV1200 confocal microscope (further described in "Materials and methods").

Qualitative assessment of immunohistochemical staining

To assess the effect of the decalcification process on immunohistochemical staining we examined CGRP, TH, CD31, NGF, TrkA and p75 staining in tissue sections obtained from; non-decalcified young bone and decalcified young, adult and aging bone. Sections were examined under an Olympus FV1200 confocal microscope using a 60x objective, under which it was possible to distinguish individual nerve fibers. The bone marrow and periosteum region of the distal end of the femur was selected for evaluation due to the ease at which nerve fiber structures could be visualized in this compartment (bone marrow) and the density of nerve fibers (periosteum). Two 60x objective fields of the marrow per animal from 5 animals per group were used for evaluation. We used a scale of – to +++ for qualitative assessment of immunohistochemical staining of nerve fibers. The – indicates no detectable signal; + = minimal signal, requires significant increase in laser power to visualize; ++ = average staining signal, requires minimal increase in laser power to visualize; +++ = maximum staining signal, requires no increase in laser power to visualize.

Statistical Analysis

All values are expressed as means ± SEM. Comparison of data for the young, adult and aging mice were analyzed using 2-factor ANOVA, followed by Tukey's multiple comparisons test with adjusted P values. Student's t-test was used when comparing 2 means. Significance level was set at $p \leq 0.05$. All statistical analyses were performed using Prism (GraphPad, La Jolla, CA).

RESULTS

Histologic comparison of femurs from young (10 days), adult (3 months) and aging (24 months) animals

Across the three examined age groups, young (10 days), adult (3 months) and aging (24 months) there were noticeable histologic differences. Histological analysis of the femur using Safranin O, a stain for cartilage (red) and mineralization (blue), revealed that the young bone was still undergoing mineralization as illustrated by the extensive presence of cartilage throughout the distal head (Fig. 1A). Adult and aging femurs had fully mineralized and displayed hallmarks of a mature femur, closure of the growth plate and fully formed

trabecular bone (Fig. 1B, C). Additionally, the young bone was approximately 1/4 the size of the adult and aging bone.

Morphologic and neuronal characteristics of the young, adult and aging periosteum

The periosteum can be divided into two distinct regions, the outer fibrous layer and the inner cambium layer. In the present study, we found that in young, adult and aging animals, the thickness of the cambium layer was 56±2, 20±1 and 6±0.25 microns respectively (Fig. 2A, B & C, respectively). The morphology of the two periosteal layers was confirmed using confocal microscopy and DAPI counterstaining. In addition to the decline in the thickness of the cambium layer with age, we observed a decline in the thickness of the fibrous layer as well between the young and adult periosteum, 76±2 vs. 24±1 microns, respectively. There was no change in fibrous thickness when comparing the adult and aging periosteum, 24±1 vs. 23±2 microns, respectively.

To investigate the sensory and sympathetic innervation of the periosteum, frozen bone sections from young, adult and aging femurs were labeled with fluorescent antibodies raised against primary antibodies for: calcitonin gene-related peptide (CGRP), a marker for peptide-rich C-fibers and some A-delta sensory nerve fibers and tyrosine hydroxylase (TH), a marker for sympathetic nerve fibers. Additionally, we looked at the vascularization of this compartment using CD31, a marker for endothelial cells (Fig. 2). Differential interference contrast (DIC) microscopy was used to show the cortical bone and for orientation purposes. Qualitative analysis revealed that the young periosteum had the highest total number of CGRP+ and TH+ nerve fibers compared to the adult and aging periosteum (Fig. 2A), with the aging periosteum having the lowest amount of sensory and sympathetic nerve fibers (Fig. 2C). Interestingly, when comparing the density of CGRP and TH in the three age groups, the young animals had a significantly lower density ($p < 0.05$) of CGRP+ (2261±442 mm/mm^3) and TH+ (995±200 mm/mm^3) nerve fibers compared to adult (CGRP+: 3723±474 mm/mm^3; TH+: 2796±416 mm/mm^3) and aging (CGRP+: 3574±310 mm/mm^3; TH+ 3750±260 mm/mm^3) animals. This seemingly contradictory finding can be explained by noting that the thickness of the periosteum shrinks with age with relative thickness of young, adult and aging cambium layer being 12:4:1, respectively.

Similar to other studies, we show that the sensory and sympathetic nerve fibers in the periosteum have distinctive morphologies. TH+ sympathetic fibers have a “corkscrew” morphology and are typically found wrapping around blood vessels in the outer cambium layer which is adjacent to the outer fibrous layer (Fig. 2A, B). On the other hand, CGRP+ sensory fibers display a more linear pattern along the long axis of the femur and are usually found immediately adjacent to cortical bone within the cambium layer (Fig 2A, B, C). Furthermore, we observed that both sensory and sympathetic nerve fibers predominately innervated the cambium layer versus the fibrous layer (data not included).

CGRP+ sensory and TH+ sympathetic innervation of Haversian canals in the cortical bone of the adult and aging femur

A combination of confocal and bright field microscopy was used to characterize the sensory and sympathetic innervation of cortical bone in young, adult and aging femurs (Fig. 3).

CGRP+ sensory and TH+ sympathetic fibers were exclusively observed in Haversian canals. Haversian canals were not noted in young animals, as the largely cartilaginous bone had yet to form canals, which are an indication of the formation of mature, compact bone. Not all Haversian canals were vascularized (i.e. contained CD31+ blood vessels) and significantly more ($p < 0.05$) canals were vascularized in the adult femur compared to aging animals, 89±3% versus 62±3%, respectively. Similar to the periosteum and bone marrow, TH+ sympathetic fibers in cortical bone had a cylindrical morphology and wrapped around CD31+ endothelial vessels. CGRP+ sensory fibers were also found in the canals, in close proximity to blood vessels and had a linear appearance. Approximately 26% of all Haversian canals were innervated by CGRP+ nerve fibers in both the adult and aging cortical bone (Fig. 3B, C). Interestingly, we observed a significant decline in the percentage of canals innervated by TH+ sympathetic fibers, 48±5% versus 14±2% in the adult and aging animal, respectively (Fig. E, F). As previously stated, no Haversian canals were found in young cortical bone though we did observe occasional lone sensory (Fig. 3A) and sympathetic (Fig. 3D) nerve fiber innervation of this bone compartment at this age. It should be noted that we did observe a significant difference ($p < 0.05$) in the percentage of canals in the adult (8±1%) and aging (3±1%) that had either CGRP+ and/or TH+ nerve fibers but did not contain CD31+ blood vessels.

CGRP+ sensory and TH+ sympathetic innervation of the bone marrow

In the bone marrow of the young, adult and aging femur CGRP+ sensory nerve fibers exhibited a relatively linear morphology in the marrow of all examined age groups (Fig. 4A, B, C). The young bone marrow (576±39 mm/mm^3) had a slightly higher CGRP+ sensory nerve density/unit area compared to the adult (344±7 mm/mm^3) and aging (343±16 mm/mm^3) bone marrow, but both these differences were not statistically significant. High power images of CGRP+ sensory structures in the marrow revealed their branching patterns (Fig. 4D, E, F) which was seen in all aspect of the bone marrow. TH+ sympathetic fibers in the marrow demonstrated a distinctive cylindrical morphology (Fig. 4G, H, I) and although there was a small increase in TH+ sympathetic nerve fiber density/unit area with age (young: 376±48 mm/mm^3; adult: 461±53 mm/mm^3; aging: 518±52 mm/mm^3) these differences were not statistically significant.

Immunohistochemical staining of nerve fibers in non-decalcified and decalcified bone

The decalcification of calcified bone requires using chemicals like Ethylenediaminetetraacetic acid (EDTA) before the bone is processed for immunohistochemistry. However, few studies have investigated the effects of these chemicals on the retention of neurologic markers post-decalcification. CGRP+ sensory fibers and tropomyosin-related kinase receptor A+ (TrkA), the cognate receptor of nerve growth factor (NGF), were examined in the marrow and periosteum of young non-decalcified and decalcified femurs (Fig 5). We selected young tissue because at this stage of development, the femur is only partially mineralized allowing for easy sectioning of the femur without decalcification. CGRP immunostaining was robust in both tissue compartments regardless of whether the tissue had undergone decalcification (Fig. 5A, B). However, the decalcification process negatively affected the robustness of TrkA immunostaining in both the periosteum and bone marrow (Fig. 5C, D). In addition to the

CGRP and TrkA neuronal markers, we examined the effects of decalcification on various other neuronal markers (Table 2). What is interesting is that the negative effects of decalcification were antigen specific, in that some markers like CGRP, TH and CD31 were unaffected by the decalcification process while others like TrkA, p75 and NGF were significantly affected by the process (Table 2).

DISCUSSION

Changes in the sensory and sympathetic innervation of the skeleton across the lifespan

In examining the femur of young, adult and aging mice, it is clear that remarkable changes occur in both the bone and cartilage over the lifespan (Manolagas and Parfitt 2010). The most obvious change is simply the size of the femur as the young 10-day old mouse femur is approximately 1/4 the length of the adult or aging femur. A second major change is in the extent of bone calcification, as the cortical wall of the young femur is almost completely cartilaginous and non-calcified whereas the adult and aging cortical bone is highly calcified. A third major change is the age-related decline in the thickness of the cambium layer of the periosteum which is accompanied by a concomitant reduction in the proliferation of osteo-progenitor cells (Thompson, Chartier et al. 2016). In the young mouse femur, the cambium layer of the periosteum is 56 microns thick, in the adult it is 20 microns thick and in the aging mouse it is 6 microns thick. Similar age-related decline in the thickness of the periosteum have been observed in the rabbit and human bone (O'Driscoll, Saris et al. 2001, Seeman 2003, Allen, Hock et al. 2004). Other changes that are evident when comparing the adult vs. the aging femur are that compared to the adult, in the aging femur; the cortical wall becomes thinner, trabeculae are fewer in number, the marrow has many more adipose deposits, and the articular cartilage of the knee becomes thinner and more calcified (Exton-Smith, Millard et al. 1969, Firooznia, Golimbu et al. 1984, Ferguson, Ayers et al. 2003, Manolagas and Parfitt 2010).

Considering the number of changes that occur in bone and articular cartilage over the lifespan, one might expect a dramatic decline in the sensory and sympathetic innervation of the femur. However, while there clearly is a marked decline in the overall number of sensory and sympathetic nerve fibers in the periosteum and sympathetic nerves in cortical bone with aging, the general morphology and organization of the nerves remains remarkably similar. Thus, although the cambium layer of the periosteum undergoes a 10-fold decrease in thickness with age with a clear loss in the overall number of sensory and sympathetic nerve fibers, the general organization remains the same with there being CD31+ blood vessels, CGRP+ sensory nerve fibers and TH+ sympathetic fibers in the cambium layer, even in the greatly thinned aging periosteum. Similarly, in comparing the adult vs. aging cortical bone, while there is a decline in the percent of CD31+ Haversian canals that contain blood vessels (89% vs. 62%) the percent of CD31+ Haversian canals that are innervated by CGRP+ sensory fibers do not decline whereas there is a marked decline in CD31+ Haversian canals that are innervated by TH+ sympathetic nerve fibers with age. Interestingly, in the cortical wall of the young femur (which is largely cartilaginous, avascular and has no CD31+ endothelial cells as the Haversian canals have yet to form) one still finds occasional CGRP+ and TH+ nerve fibers in this structure. Similarly, although the presence of adipose deposits

in the bone marrow is much more prevalent in the aging vs. the young or adult femur (Ferguson, Ayers et al. 2003), there is not a significant difference in the density of innervation by CGRP+ and TH+ nerve fibers in the bone marrow when comparing the young, adult and aging femur. Lastly, no sensory fibers, sympathetic fibers, or CD31+ blood vessels were ever detected in the articular cartilage of the knee joint in the young, adult or aging femur.

Mechanisms that drive skeletal pain across the lifespan

The present findings suggest that sensory nerve fibers that are involved in detecting noxious stimuli in the skeleton are present across the lifespan of the animal. In light of this observation, a major question is whether similar peripheral mechanisms drive skeletal pain in the young, adult and aging skeleton? While in many ways this is a difficult question to address, as pain is a subjective experience, a variety of clinical studies have suggested that many therapies that are effective in relieving skeletal pain in the adult or aging animal may be effective at relieving skeletal pain in the young. One of the best examples of this are the bisphosphonates and Denosumab which were originally shown to reduce bone cancer in adults by inhibition of osteoclast induced acidosis. More recently, it has been shown that bisphosphonates or Denosumab can also markedly attenuate skeletal pain in neonatal and pediatric patients with osteogenesis imperfecta, juvenile Paget's disease, fibrous dysplasia, and aneurysmal bone cyst (Boyce, 2017). Mechanistically this makes sense as the present study clearly shows that there are many CGRP+ sensory nerve fibers innervating the young, adult and aging bone. Previous work has shown that many CGRP+ fibers also express acid sensing ion channels such as TRPV1, ASIC-1 and ASIC-3 (Gajda, Litwin et al. 2005, Mantyh 2014) and these ion channels are known to be activated by the extracellular pH of 4 that is generated by osteoclasts. These data suggest that if excessive osteoclast induced acidosis is present, whether it be in young, adult or aging patients, blocking this acidosis can attenuate skeletal pain.

A second common mechanism which probably drives pain in the young, adult and aged skeleton is stimulation of mechanosensitive nociceptors that innervate the periosteum, cortical bone and bone marrow. Previous studies have shown that many of the sensory nerve fibers that innervate the periosteum and cortical bone are mechanosensitive nociceptors that rapidly respond to mechanical distortion of either the periosteum and/or the underlying cortical bone (Inman and deC. M. Saunders 1944, Sakada and Taguchi 1971, Mahns, Ivanusic et al. 2006, Zhao and Levy 2014, Nencini and Ivanusic 2016). Similarly, increased intraosseous pressure in the bone marrow will stimulate mechanosensitive nociceptors that innervate the bone marrow (Furusawa 1970, Seike 1976, Haegerstam 2001, Nencini and Ivanusic 2017). As many genetic diseases involving bone and cartilage result in relatively weak bone, normal loading of a weakened bone would be expected to result in pain due to distortion of the mechanosensitive sensory nerve fibers that densely innervate the young, adult and aging bone.

A third mechanism that appears to drive skeletal pain in the young, adult and aging bone and joint, is the release of inflammatory mediators that occurs in disease or following injury of bone and/or cartilage. Several mediators including prostaglandins, bradykinin, endothelins,

and nerve growth factor (Mantyh 2014, Nencini and Ivanusic 2016, Nencini, Ringuet et al. 2017) all have been shown to excite and/or sensitize nociceptors that innervate the skeleton. Therapies targeting these mediators have been shown to relieve pain in a variety of human skeletal pathologies or diseases, including osteoarthritis (Schnitzer, Lane et al. 2011, Seidel and Lane 2012, Seidel, Wise et al. 2013, Tiseo, Kivitz et al. 2014), low back pain (Katz, Borenstein et al. 2011, Kivitz, Gimbel et al. 2013), and bone cancer pain (Sopata, Katz et al. 2015, Majuta, Guedon et al. In Press). Presumably, blockade of NGF will be contraindicated in young patients with skeletal pain as NGF is involved in the growth and survival of the developing sensory and sympathetic nervous system in the young. However, many individuals with genetic disorders of the bone and joint (such as fibrous dysplasia) not only have significant pain when they are young but continue to have chronic skeletal pain throughout their adult life (Chapurlat, Gensburger et al. 2012). Whether targeting blockage of NGF or its cognate receptor TrkA will block pain in adults with genetic disorders of the bone and joints has yet to be determined.

The fourth mechanism that may be involved in driving skeletal pain is ectopic nerve sprouting. Following injury or disease, several neurotrophic factors including NGF are released by stromal and inflammatory cells and can induce an exuberant and highly ectopic sprouting resulting in hyper-innervation of the marrow, mineralized bone and periosteum (Mantyh 2014). Importantly, NGF not only induces ectopic nerve sprouting into areas of bone that are normally poorly innervated, but also sensitizes TrkA+ nociceptors (Woolf, Safieh-Garabedian et al. 1994, Dyck, Peroutka et al. 1997, Ma and Woolf 1997, Ueda, Hirose et al. 2002, Svensson, Cairns et al. 2003, Pezet and McMahon 2006, Rukwied, Mayer et al. 2010, Nencini, Ringuet et al. 2017) so that even normally non-noxious loading or movement of the bone is perceived as a highly noxious event. Skeletal diseases where ectopic sprouting has been observed are bone cancer (Jimenez-Andrade, Bloom et al. 2010, Mantyh, Jimenez-Andrade et al. 2010, Bloom, Jimenez-Andrade et al. 2011), unhealed bone fractures (Hukkanen, Konttinen et al. 1992, Chartier, Thompson et al. 2014), osteoarthritis (Walsh, McWilliams et al. 2010, Jimenez-Andrade and Mantyh 2012, Driscoll, Chanalaris et al. 2016), and the degenerated vertebral disc (Johnson, Caterson et al. 2002, Johnson, Caterson et al. 2005, Tolofari, Richardson et al. 2010). Once this ectopic nerve sprouting has occurred, mechanical strain and/or distortion of a weakened bone or joint may result in normally innocuous movement and loading of the bone now being perceived as a noxious event. Whether significant and unwanted sprouting of sensory and sympathetic nerve fibers also occurs in young patients with genetic disorders of the skeleton has yet to be determined, but if it does occur, it may provide insight into the mechanisms that drive the transition from acute to chronic skeletal pain in these patients (Holley, Wilson et al. 2017).

The normally highly restricted innervation of the young, adult and aging femur may change following injury or disease

Two of the most remarkable aspects of the present study are just how richly innervated the young bone is and how restricted and regulated the location, density and morphology of sensory and sympathetic nerve fibers is throughout the lifespan. Thus, across the lifespan, the areas of bone and joint with the highest density of sensory and sympathetic nerve fibers remains the same: periosteum > marrow > cortical bone > articular cartilage. Even within

each compartment of bone there is tight regulation in terms of density, phenotype and morphology such that in the periosteum > 90% of nerve fibers are in the cambium, with fewer than 10% being present in the fibrous layer. In adult and aging cortical bone the great majority of sensory and sympathetic nerve fibers are only found in vascularized CD31+ Haversian canals. In the bone marrow, the sensory nerve fibers are linear in appearance, whereas the sympathetic nerve fibers nearly always have a “corkscrew” shaped pattern and tightly wrap around CD31+ blood vessels.

Currently, we know relatively little about the specific molecules and mechanisms that coordinate the growth, sprouting and maintenance of sensory and sympathetic nerve fibers in bone and cartilage (Ivanusic 2009, Jimenez-Andrade, Bloom et al. 2010, Aso, Ikeuchi et al. 2014, Nencini, Ringuet et al. 2017). Molecules that have been implicated in regulating these processes include NGF and members of the netrin, semaphorin, integrin, FGF and VEGF family (Voyvodic 1987, Graef, Wang et al. 2003, Jimenez-Andrade, Mantyh et al. 2010, Bloom, Jimenez-Andrade et al. 2011, Ascano, Bodmer et al. 2012, Krock, Rosenzweig et al. 2014, Selvaraj, Gangadharan et al. 2015, Kuner and Flor 2016, Nencini, Ringuet et al. 2017). However, what specific cell types synthesize and release these growth factors, how the expression of these factors changes due to injury, disease or aging, and whether the phenotype and response characteristics of sensory and sympathetic nerve fibers that innervate the skeleton change across the lifespan remains largely unknown. Understanding the interplay between bone cells and nerves across the lifespan may provide insights into how nerves participate in driving age related changes in bone and cartilage (Elefteriou, Campbell et al. 2014) and how changes in bone and cartilage drive skeletal pain across the lifespan.

Conclusions and limitations

The present study suggests that the young, adult and aging mouse femur, the periosteum, cortical bone and bone marrow are all innervated by sensory and sympathetic nerve fibers. The compartments of bone that had the highest density of nerve fibers/unit area remained the same in the young, adult and aging femur (i.e. periosteum > marrow > cortical bone) with no nerve fibers being observed in the articular cartilage at any age. These results suggest while there is a significant decline in both sensory and sympathetic innervation of the skeleton with age, the anatomical substrates required for detection of noxious stimuli and the efferent modulation of bone and joint are present in the young, adult and aging skeleton. Limitations of the study are that the analysis was only performed on the normal male mouse femur and only antigens that showed little loss of antigenicity following decalcification were examined.

Acknowledgments

This research was supported by the National Institutes of Health (grant numbers CA154550, CA157449, and NS023970) to Patrick Mantyh. Dr. Mantyh has served as a consultant and/or received research grants from Abbott (Abbott Park, IL), Adolor (Exton, PA), Array Biopharma (Boulder, CO), Johnson and Johnson (New Brunswick, NJ), Merck (White Plains, New York), Pfizer (New York, NY), Plexxikon (Berkeley, CA), Rinat (South San Francisco, CA), and Roche (Palo Alto, CA).

References

Allen MR, Hock JM, Burr DB. Periosteum: biology, regulation, and response to osteoporosis therapies. Bone. 2004; 35(5):1003–1012. [PubMed: 15542024]

Arnold W. Immunohistochemical investigation of the human inner ear. Limitations and prospects. Acta Otolaryngol. 1988; 105(5–6):392–397. [PubMed: 3041735]

Ascano M, Bodmer D, Kuruvilla R. Endocytic trafficking of neurotrophins in neural development. Trends Cell Biol. 2012; 22(5):266–273. [PubMed: 22444728]

Aso K, Ikeuchi M, Izumi M, Sugimura N, Kato T, Ushida T, Tani T. Nociceptive phenotype of dorsal root ganglia neurons innervating the subchondral bone in rat knee joints. Eur J Pain. 2014; 18(2): 174–181. [PubMed: 23821557]

Bloom AP, Jimenez-Andrade JM, Taylor RN, Castaneda-Corral G, Kaczmarska MJ, Freeman KT, Coughlin KA, Ghilardi JR, Kuskowski MA, Mantyh PW. Breast cancer-induced bone remodeling, skeletal pain, and sprouting of sensory nerve fibers. J Pain. 2011; 12(6):698–711. [PubMed: 21497141]

Boyce AM. Denosumab: an Emerging Therapy in Pediatric Bone Disorders. Curr Osteoporos Rep. 2017; 15(4):283–292. [PubMed: 28643220]

Boyce AM, Chong WH, Yao J, Gafni RI, Kelly MH, Chamberlain CE, Bassim C, Cherman N, Ellsworth M, Kasa-Vubu JZ, Farley FA, Molinolo AA, Bhattacharyya N, Collins MT. Denosumab treatment for fibrous dysplasia. J Bone Miner Res. 2012; 27(7):1462–1470. [PubMed: 22431375]

Brandi ML, Collin-Osdoby P. Vascular biology and the skeleton. J Bone Miner Res. 2006; 21(2):183–192. [PubMed: 16418774]

Chapurlat RD, Gensburger D, Jimenez-Andrade JM, Ghilardi JR, Kelly M, Mantyh P. Pathophysiology and medical treatment of pain in fibrous dysplasia of bone. Orphanet J Rare Dis. 2012; 7(Suppl 1):S3. [PubMed: 22640953]

Chartier SR, Thompson ML, Longo G, Fealk MN, Majuta LA, Mantyh PW. Exuberant sprouting of sensory and sympathetic nerve fibers in nonhealed bone fractures and the generation and maintenance of chronic skeletal pain. Pain. 2014; 155(11):2323–2336. [PubMed: 25196264]

Chawla S, Henshaw R, Seeger L, Choy E, Blay JY, Ferrari S, Kroep J, Grimer R, Reichardt P, Rutkowski P, Schuetze S, Skubitz K, Staddon A, Thomas D, Qian Y, Jacobs I. Safety and efficacy of denosumab for adults and skeletally mature adolescents with giant cell tumour of bone: interim analysis of an open-label, parallel-group, phase 2 study. Lancet Oncol. 2013; 14(9):901–908. [PubMed: 23867211]

Clinch J, Eccleston C. Chronic musculoskeletal pain in children: assessment and management. Rheumatology. 2009:kep001.

Driscoll C, Chanalaris A, Knights C, Ismail H, Sacitharan PK, Gentry C, Bevan S, Vincent TL. Nociceptive Sensitizers Are Regulated in Damaged Joint Tissues, Including Articular Cartilage, When Osteoarthritic Mice Display Pain Behavior. Arthritis Rheumatol. 2016; 68(4):857–867. [PubMed: 26605536]

Dyck PJ, Peroutka S, Rask C, Burton E, Baker MK, Lehman KA, Gillen DA, Hokanson JL, O'Brien PC. Intradermal recombinant human nerve growth factor induces pressure allodynia and lowered heat-pain threshold in humans. Neurology. 1997; 48(2):501–505. [PubMed: 9040746]

Elefteriou F, Campbell P, Ma Y. Control of bone remodeling by the peripheral sympathetic nervous system. Calcif Tissue Int. 2014; 94(1):140–151. [PubMed: 23765388]

Exton-Smith AN, Millard PH, Payne PR, Wheeler EF. Pattern of development and loss of bone with age. Lancet. 1969; 2(7631):1154–1157. [PubMed: 4187198]

Ferguson VL, Ayers RA, Bateman TA, Simske SJ. Bone development and age-related bone loss in male C57BL/6J mice. Bone. 2003; 33(3):387–398. [PubMed: 13678781]

Firooznia H, Golimbu C, Rafii M, Schwartz MS, Alterman ER. Quantitative computed tomography assessment of spinal trabecular bone. II. In osteoporotic women with and without vertebral fractures. J Comput Tomogr. 1984; 8(2):99–103. [PubMed: 6713933]

Freeman KT, Koewler NJ, Jimenez-Andrade JM, Buus RJ, Herrera MB, Martin CD, Ghilardi JR, Kuskowski MA, Mantyh PW. A fracture pain model in the rat: adaptation of a closed femur

fracture model to study skeletal pain. Anesthesiology. 2008; 108(3):473–483. [PubMed: 18292685]

Furusawa S. A neurophysiological study on the sensibility of the bone marrow. Nihon Seikeigeka Gakkai Zasshi. 1970; 44(5):365–370. [PubMed: 5466754]

Gajda M, Litwin JA, Cichocki T, Timmermans JP, Adriaensen D. Development of sensory innervation in rat tibia: co-localization of CGRP and substance P with growth-associated protein 43 (GAP-43). J Anat. 2005; 207(2):135–144. [PubMed: 16050900]

Gossai N, Hilgers MV, Polgreen LE, Greengard EG. Critical hypercalcemia following discontinuation of denosumab therapy for metastatic giant cell tumor of bone. Pediatr Blood Cancer. 2015; 62(6): 1078–1080. [PubMed: 25556556]

Graef IA, Wang F, Charron F, Chen L, Neilson J, Tessier-Lavigne M, Crabtree GR. Neurotrophins and netrins require calcineurin/NFAT signaling to stimulate outgrowth of embryonic axons. Cell. 2003; 113(5):657–670. [PubMed: 12787506]

Grasemann C, Schundeln MM, Hovel M, Schweiger B, Bergmann C, Herrmann R, Wieczorek D, Zabel B, Wieland R, Hauffa BP. Effects of RANK-ligand antibody (denosumab) treatment on bone turnover markers in a girl with juvenile Paget's disease. J Clin Endocrinol Metab. 2013; 98(8): 3121–3126. [PubMed: 23788687]

Haegerstam GA. Pathophysiology of bone pain: a review. Acta Orthop Scand. 2001; 72(3):308–317. [PubMed: 11480611]

Hayat M. Factors Affecting Antigen Retrieval. Microscopy, Immunohistochemistry, and Antigen Retrieval Methods: For Light and Electron Microscopy. 2002:71–93.

Heaney RP, Abrams S, Dawson-Hughes B, Looker A, Marcus R, Matkovic V, Weaver C. Peak bone mass. Osteoporos Int. 2000; 11(12):985–1009. [PubMed: 11256898]

Holley AL, Wilson AC, Palermo TM. Predictors of the transition from acute to persistent musculoskeletal pain in children and adolescents: a prospective study. Pain. 2017; 158(5):794–801. [PubMed: 28151835]

Hoyer-Kuhn H, Semler O, Schoenau E. Effect of denosumab on the growing skeleton in osteogenesis imperfecta. J Clin Endocrinol Metab. 2014; 99(11):3954–3955. [PubMed: 25148238]

Hukkanen M, Konttinen YT, Rees RG, Santavirta S, Terenghi G, Polak JM. Distribution of nerve endings and sensory neuropeptides in rat synovium, meniscus and bone. Int J Tissue React. 1992; 14(1):1–10.

Hukkanen M, Konttinen YT, Santavirta S, Paavolainen P, Gu XH, Terenghi G, Polak JM. Rapid proliferation of calcitonin gene-related peptide-immunoreactive nerves during healing of rat tibial fracture suggests neural involvement in bone growth and remodelling. Neuroscience. 1993; 54(4): 969–979. [PubMed: 8341427]

Inman VT, J B, de Saunders CM. Referred Pain From Skeletal Structures. The Journal of Nervous and Mental Disease. 1944; 99(5):660–667.

Ivanusic JJ. Size, neurochemistry, and segmental distribution of sensory neurons innervating the rat tibia. J Comp Neurol. 2009; 517(3):276–283. [PubMed: 19757492]

Jimenez-Andrade JM, Bloom AP, Mantyh WG, Koewler NJ, Freeman KT, Delong D, Ghilardi JR, Kuskowski MA, Mantyh PW. Capsaicin-sensitive sensory nerve fibers contribute to the generation and maintenance of skeletal fracture pain. Neuroscience. 2009; 162(4):1244–1254. [PubMed: 19486928]

Jimenez-Andrade JM, Bloom AP, Stake JI, Mantyh WG, Taylor RN, Freeman KT, Ghilardi JR, Kuskowski MA, Mantyh PW. Pathological sprouting of adult nociceptors in chronic prostate cancer-induced bone pain. J Neurosci. 2010; 30(44):14649–14656. [PubMed: 21048122]

Jimenez-Andrade JM, Mantyh PW. Sensory and sympathetic nerve fibers undergo sprouting and neuroma formation in the painful arthritic joint of geriatric mice. Arthritis Res Ther. 2012; 14(3):R101. [PubMed: 22548760]

Jimenez-Andrade JM, Mantyh WG, Bloom AP, Xu H, Ferng AS, Dussor G, Vanderah TW, Mantyh PW. A phenotypically restricted set of primary afferent nerve fibers innervate the bone versus skin: therapeutic opportunity for treating skeletal pain. Bone. 2010; 46(2):306–313. [PubMed: 19766746]

Jimenez-Andrade JM, Martin CD, Koewler NJ, Freeman KT, Sullivan LJ, Halvorson KG, Barthold CM, Peters CM, Buus RJ, Ghilardi JR, Lewis JL, Kuskowski MA, Mantyh PW. Nerve growth factor sequestering therapy attenuates non-malignant skeletal pain following fracture. Pain. 2007; 133(1–3):183–196. [PubMed: 17693023]

Johnson WE, Caterson B, Eisenstein SM, Hynds DL, Snow DM, Roberts S. Human intervertebral disc aggrecan inhibits nerve growth in vitro. Arthritis Rheum. 2002; 46(10):2658–2664. [PubMed: 12384924]

Johnson WE, Caterson B, Eisenstein SM, Roberts S. Human intervertebral disc aggrecan inhibits endothelial cell adhesion and cell migration in vitro. Spine (Phila Pa 1976). 2005; 30(10):1139–1147. [PubMed: 15897827]

Karras NA, Polgreen LE, Ogilvie C, Manivel JC, Skubitz KM, Lipsitz E. Denosumab treatment of metastatic giant-cell tumor of bone in a 10-year-old girl. J Clin Oncol. 2013; 31(12):e200–202. [PubMed: 23509309]

Katz N, Borenstein DG, Birbara C, Bramson C, Nemeth MA, Smith MD, Brown MT. Efficacy and safety of tanezumab in the treatment of chronic low back pain. Pain. 2011; 152(10):2248–2258. [PubMed: 21696889]

Kivitz AJ, Gimbel JS, Bramson C, Nemeth MA, Keller DS, Brown MT, West CR, Verburg KM. Efficacy and safety of tanezumab versus naproxen in the treatment of chronic low back pain. Pain. 2013; 154(7):1009–1021. [PubMed: 23628600]

Koewler NJ, Freeman KT, Buus RJ, Herrera MB, Jimenez-Andrade JM, Ghilardi JR, Peters CM, Sullivan LJ, Kuskowski MA, Lewis JL, Mantyh PW. Effects of a monoclonal antibody raised against nerve growth factor on skeletal pain and bone healing after fracture of the C57BL/6J mouse femur. J Bone Miner Res. 2007; 22(11):1732–1742. [PubMed: 17638576]

Krock E, Rosenzweig DH, Chabot-Dore AJ, Jarzem P, Weber MH, Ouellet JA, Stone LS, Haglund L. Painful, degenerating intervertebral discs up-regulate neurite sprouting and CGRP through nociceptive factors. J Cell Mol Med. 2014; 18(6):1213–1225. [PubMed: 24650225]

Kruger L, Silverman JD, Mantyh PW, Sternini C, Brecha NC. Peripheral patterns of calcitonin-gene-related peptide general somatic sensory innervation: cutaneous and deep terminations. J Comp Neurol. 1989; 280(2):291–302. [PubMed: 2784448]

Kuner R, Flor H. Structural plasticity and reorganisation in chronic pain. Nat Rev Neurosci. 2016; 18(1):20–30. [PubMed: 27974843]

Lange T, Stehling C, Frohlich B, Klingenhofer M, Kunkel P, Schneppenheim R, Escherich G, Gosheger G, Hardes J, Jurgens H, Schulte TL. Denosumab: a potential new and innovative treatment option for aneurysmal bone cysts. Eur Spine J. 2013; 22(6):1417–1422. [PubMed: 23455951]

Ma QP, Woolf CJ. The progressive tactile hyperalgesia induced by peripheral inflammation is nerve growth factor dependent. Neuroreport. 1997; 8(4):807–810. [PubMed: 9141043]

Mach DB, Rogers SD, Sabino MC, Luger NM, Schwei MJ, Pomonis JD, Keyser CP, Clohisy DR, Adams DJ, O'Leary P, Mantyh PW. Origins of skeletal pain: sensory and sympathetic innervation of the mouse femur. Neuroscience. 2002; 113(1):155–166. [PubMed: 12123694]

Mahns DA, Ivanusic JJ, Sahai V, Rowe MJ. An intact peripheral nerve preparation for monitoring the activity of single, periosteal afferent nerve fibres. J Neurosci Methods. 2006; 156(1–2):140–144. [PubMed: 16574241]

Majuta LA, Guedon J-MG, Mitchell SAT, Kuskowski MA, Mantyh PW. Mice with cancer-induced bone pain show a marked decline in day/night activity. PAIN Reports. (In Press). Latest Articles.

Manolagas SC, Parfitt AM. What old means to bone. Trends in Endocrinology & Metabolism. 2010; 21(6):369–374. [PubMed: 20223679]

Mantyh PW. The neurobiology of skeletal pain. Eur J Neurosci. 2014; 39(3):508–519. [PubMed: 24494689]

Mantyh WG, Jimenez-Andrade JM, Stake JI, Bloom AP, Kaczmarska MJ, Taylor RN, Freeman KT, Ghilardi JR, Kuskowski MA, Mantyh PW. Blockade of nerve sprouting and neuroma formation markedly attenuates the development of late stage cancer pain. Neuroscience. 2010; 171(2):588–598. [PubMed: 20851743]

Martin-Broto J, Cleeland CS, Glare PA, Engellau J, Skubitz KM, Blum RH, Ganjoo KN, Staddon A, Dominkus M, Feng A, Qian Y, Braun A, Jacobs I, Chung K, Atchison C. Effects of denosumab on pain and analgesic use in giant cell tumor of bone: interim results from a phase II study. Acta Oncol. 2014; 53(9):1173–1179. [PubMed: 24834795]

McCarthy EF. Genetic diseases of bones and joints. Semin Diagn Pathol. 2011; 28(1):26–36. [PubMed: 21675375]

Melton LJ 3rd, Johnell O, Lau E, Mautalen CA, Seeman E. Osteoporosis and the global competition for health care resources. J Bone Miner Res. 2004; 19(7):1055–1058. [PubMed: 15176986]

Naidu A, Malmquist MP, Denham CA, Schow SR. Management of central giant cell granuloma with subcutaneous denosumab therapy. J Oral Maxillofac Surg. 2014; 72(12):2469–2484. [PubMed: 25262402]

Nencini S, Ivanusic J. Mechanically sensitive Adelta nociceptors that innervate bone marrow respond to changes in intra-osseous pressure. J Physiol. 2017; 595(13):4399–4415. [PubMed: 28295390]

Nencini S, Ivanusic JJ. The Physiology of Bone Pain. How Much Do We Really Know? Front Physiol. 2016; 7:157. [PubMed: 27199772]

Nencini S, Ringuet M, Kim DH, Chen YJ, Greenhill C, Ivanusic JJ. Mechanisms of nerve growth factor signaling in bone nociceptors and in an animal model of inflammatory bone pain. Mol Pain. 2017; 13 1744806917697011.

O'Driscoll SW, Saris DB, Ito Y, Fitzimmons JS. The chondrogenic potential of periosteum decreases with age. J Orthop Res. 2001; 19(1):95–103. [PubMed: 11332626]

Parfitt AM. Misconceptions V—activation of osteoclasts is the first step in the bone remodeling cycle. Bone. 2006; 39(6):1170–1172. [PubMed: 16963327]

Pelle DW, Ringler JW, Peacock JD, Kampfschulte K, Scholten DJ 2nd, Davis MM, Mitchell DS, Steensma MR. Targeting receptor-activator of nuclear kappaB ligand in aneurysmal bone cysts: verification of target and therapeutic response. Transl Res. 2014; 164(2):139–148. [PubMed: 24726460]

Pezet S, McMahon SB. Neurotrophins: mediators and modulators of pain. Annu Rev Neurosci. 2006; 29:507–538. [PubMed: 16776595]

Rauch F, Travers R, Plotkin H, Glorieux FH. The effects of intravenous pamidronate on the bone tissue of children and adolescents with osteogenesis imperfecta. J Clin Invest. 2002; 110(9):1293–1299. [PubMed: 12417568]

Rukwied R, Mayer A, Kluschina O, Obreja O, Schley M, Schmelz M. NGF induces non-inflammatory localized and lasting mechanical and thermal hypersensitivity in human skin. Pain. 2010; 148(3): 407–413. [PubMed: 20022698]

Sacchetti B, Funari A, Michienzi S, Di Cesare S, Piersanti S, Saggio I, Tagliafico E, Ferrari S, Robey PG, Riminucci M, Bianco P. Self-renewing osteoprogenitors in bone marrow sinusoids can organize a hematopoietic microenvironment. Cell. 2007; 131(2):324–336. [PubMed: 17956733]

Sakada S, Taguchi S. Electrophysiological studies on the free-fiber ending units of the cat mandibular periosteum. Bull Tokyo Dent Coll. 1971; 12(3):175–197. [PubMed: 5287330]

Schindelin J, Arganda-Carreras I, Frise E, Kaynig V, Longair M, Pietzsch T, Preibisch S, Rueden C, Saalfeld S, Schmid B, Tinevez JY, White DJ, Hartenstein V, Eliceiri K, Tomancak P, Cardona A. Fiji: an open-source platform for biological-image analysis. Nat Methods. 2012; 9(7):676–682. [PubMed: 22743772]

Schnitzer TJ, Lane NE, Birbara C, Smith MD, Simpson SL, Brown MT. Long-term open-label study of tanezumab for moderate to severe osteoarthritic knee pain. Osteoarthritis Cartilage. 2011; 19(6): 639–646. [PubMed: 21251985]

Schulze E, Witt M, Fink T, Hofer A, Funk RH. Immunohistochemical detection of human skin nerve fibers. Acta Histochem. 1997; 99(3):301–309. [PubMed: 9381913]

Seeman E. Periosteal bone formation–a neglected determinant of bone strength. N Engl J Med. 2003; 349(4):320–323. [PubMed: 12878736]

Seidel MF, Lane NE. Control of arthritis pain with anti-nerve-growth factor: risk and benefit. Curr Rheumatol Rep. 2012; 14(6):583–588. [PubMed: 22948388]

Seidel MF, Wise BL, Lane NE. Nerve growth factor: an update on the science and therapy. Osteoarthritis Cartilage. 2013; 21(9):1223–1228. [PubMed: 23973134]

Seike W. Electrophysiological and histological studies on the sensibility of the bone marrow nerve terminal. Yonago Acta Med. 1976; 20(3):192–211. [PubMed: 1032858]

Selvaraj D, Gangadharan V, Michalski CW, Kurejova M, Stosser S, Srivastava K, Schweizerhof M, Waltenberger J, Ferrara N, Heppenstall P, Shibuya M, Augustin HG, Kuner R. A Functional Role for VEGFR1 Expressed in Peripheral Sensory Neurons in Cancer Pain. Cancer Cell. 2015; 27(6): 780–796. [PubMed: 26058077]

Semler O, Netzer C, Hoyer-Kuhn H, Becker J, Eysel P, Schoenau E. First use of the RANKL antibody denosumab in osteogenesis imperfecta type VI. J Musculoskelet Neuronal Interact. 2012; 12(3): 183–188. [PubMed: 22947550]

Shi SR, Key ME, Kalra KL. Antigen retrieval in formalin-fixed, paraffin-embedded tissues: an enhancement method for immunohistochemical staining based on microwave oven heating of tissue sections. J Histochem Cytochem. 1991; 39(6):741–748. [PubMed: 1709656]

Sopata M, Katz N, Carey W, Smith MD, Keller D, Verburg KM, West CR, Wolfram G, Brown MT. Efficacy and safety of tanezumab in the treatment of pain from bone metastases. Pain. 2015; 156(9):1703–1713. [PubMed: 25919474]

Svensson P, Cairns BE, Wang K, Arendt-Nielsen L. Injection of nerve growth factor into human masseter muscle evokes long-lasting mechanical allodynia and hyperalgesia. Pain. 2003; 104(1–2): 241–247. [PubMed: 12855334]

Thompson ML, Chartier SR, Mitchell SA, Mantyh PW. Preventing painful age-related bone fractures: Anti-sclerostin therapy builds cortical bone and increases the proliferation of osteogenic cells in the periosteum of the geriatric mouse femur. Mol Pain. 2016; 12

Tiseo PJ, Kivitz AJ, Ervin JE, Ren H, Mellis SJ. Fasinumab (REGN475), an antibody against nerve growth factor for the treatment of pain: results from a double-blind, placebo-controlled exploratory study in osteoarthritis of the knee. Pain. 2014; 155(7):1245–1252. [PubMed: 24686255]

Tolofari SK, Richardson SM, Freemont AJ, Hoyland JA. Expression of semaphorin 3A and its receptors in the human intervertebral disc: potential role in regulating neural ingrowth in the degenerate intervertebral disc. Arthritis Res Ther. 2010; 12(1):R1. [PubMed: 20051117]

Ueda M, Hirose M, Takei N, Ibuki T, Naruse Y, Amaya F, Ibata Y, Tanaka M. Nerve growth factor induces systemic hyperalgesia after thoracic burn injury in the rat. Neurosci Lett. 2002; 328(2):97–100. [PubMed: 12133564]

Voyvodic JT. Development and regulation of dendrites in the rat superior cervical ganglion. J Neurosci. 1987; 7(3):904–912. [PubMed: 3559715]

Walsh DA, McWilliams DF, Turley MJ, Dixon MR, Franses RE, Mapp PI, Wilson D. Angiogenesis and nerve growth factor at the osteochondral junction in rheumatoid arthritis and osteoarthritis. Rheumatology (Oxford). 2010; 49(10):1852–1861. [PubMed: 20581375]

Ward L, Bardai G, Moffatt P, Al-Jallad H, Trejo P, Glorieux FH, Rauch F. Osteogenesis Imperfecta Type VI in Individuals from Northern Canada. Calcif Tissue Int. 2016; 98(6):566–572. [PubMed: 26815784]

Woolf AD, Pfleger B. Burden of major musculoskeletal conditions. Bull World Health Organ. 2003; 81(9):646–656. [PubMed: 14710506]

Woolf CJ, Safieh-Garabedian B, Ma QP, Crilly P, Winter J. Nerve growth factor contributes to the generation of inflammatory sensory hypersensitivity. Neuroscience. 1994; 62(2):327–331. [PubMed: 7530342]

Zhao J, Levy D. The sensory innervation of the calvarial periosteum is nociceptive and contributes to headache-like behavior. Pain. 2014; 155(7):1392–1400. [PubMed: 24769138]

Highlights

- There is a rich sensory and sympathetic innervation in the young bone
- With aging, there is a greater decline in sympathetic rather than sensory nerve fibers
- The preferential preservation of sensory nerve fibers suggests that nociceptors remain relatively intact with ageing

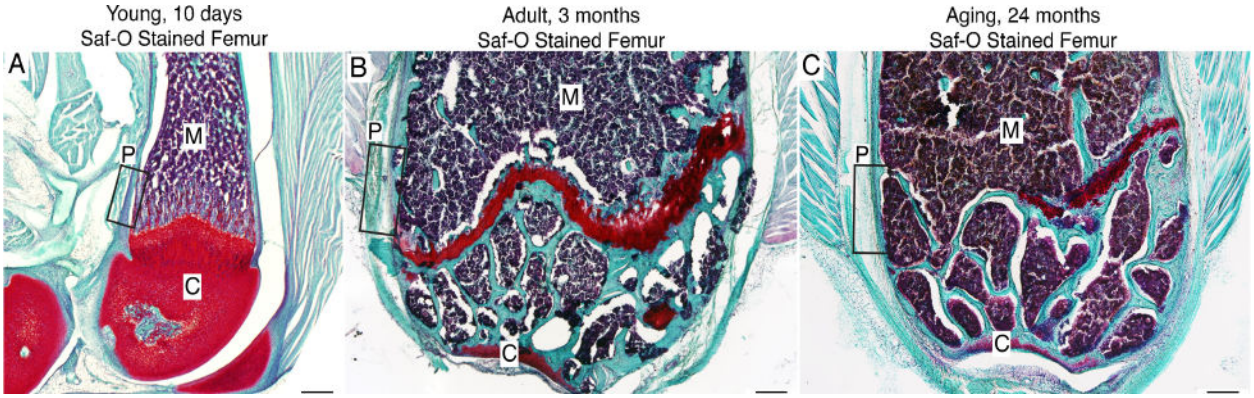

Figure 1. Tissue sections of the distal head of the young, adult and aging mouse femur stained with Safranin O

Images are light field photomicrographs of 20μm thick Safranin O (Saf-O) stained sections obtained from (A) 10 day old, (B) 3 month old and (C) 24 month old mouse femur. In these images cartilage is deep red, mineralized bone teal-blue and hemopoietic cells in bone marrow purple. In the present study, we focused on the distal end of the femur although a similar organization and age related changes were also observed in other parts of the femur. The boxes within A, B & C show where the confocal microscopy images in Figures 2–5 were acquired. Abbreviations: M, marrow; C, cartilage; P, periosteum.

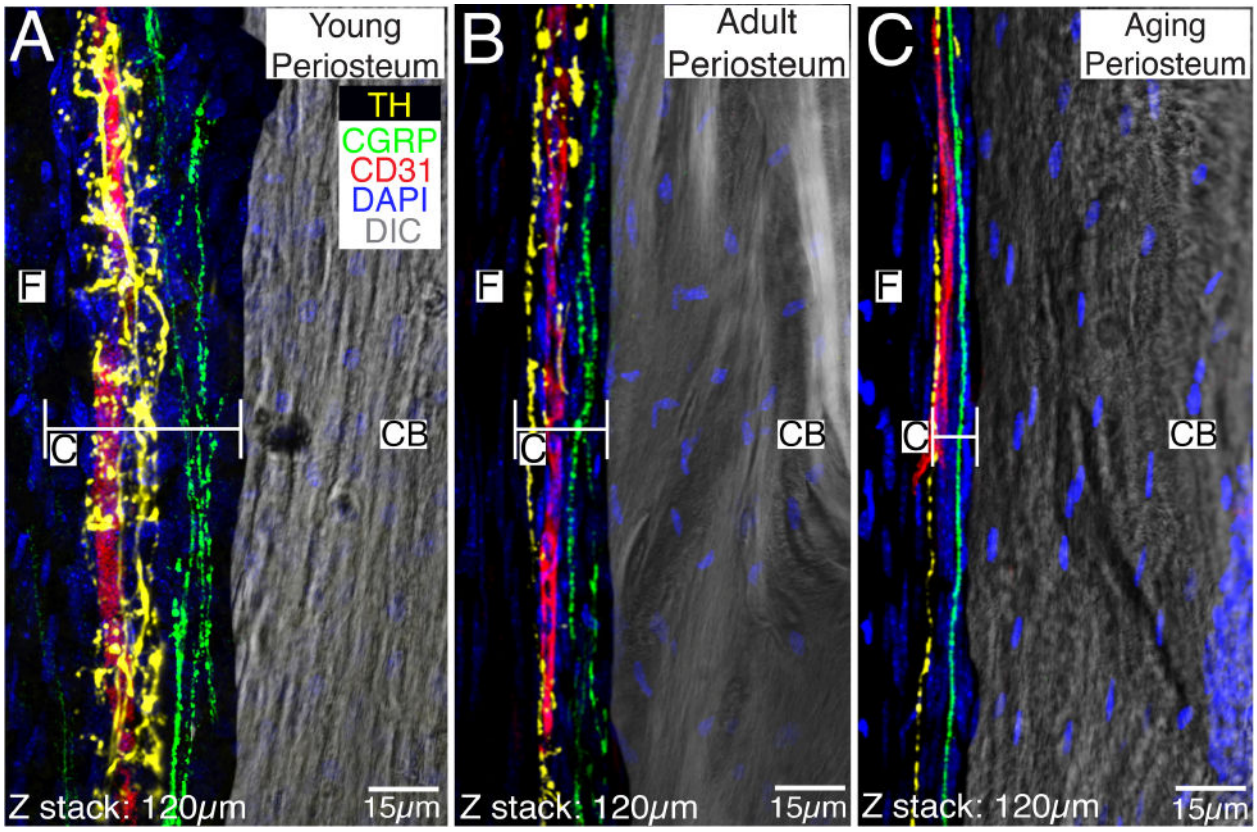

Figure 2. Localization of CD31+ blood vessels, CGRP+ primary afferent sensory nerve fibers and TH+ sympathetic nerve fibers in the periosteum of the young, adult and aging mouse femur

In images A, B and C, the periosteum and its fibrous layer (F) are in the left half of the image and the cortical bone (CB) is in the right half of the image. Note that the great majority of blood vessels and nerve fibers are present in the cambium (C) and not the fibrous (F) layer, the cambium undergoes a dramatic thinning with age, and the TH+ sympathetic nerve fibers have a distinct morphology and closer relationship to CD31+ blood vessels as compared to the CGRP+ sensory nerve fibers. Also note that even in the aging periosteum there remains CD31+ blood vessels, TH+ sympathetic nerve fibers, and CGRP+ sensory nerve fibers. In these confocal images the endothelial cells are labeled with an antibody raised against 140 kD glycoprotein known as platelet endothelial cell adhesion molecule which is also known as CD31 (red), sympathetic nerve fibers are labeled by an antibody raised against tyrosine hydroxylase (TH, yellow), and sensory nerve fibers are labeled with an antibody raised against calcitonin gene related peptide (CGRP, green). The nuclei of all cells are stained with DAPI (blue) and the image of one of the sections obtained with differential interference contrast (DIC) microscopy is included to provide orientation. Confocal images in A, B and C were obtained from two serially adjacent tissue sections. The first 60 micron serial section was stained for TH, CD31, and DAPI. The second 60 micron section was stained for CGRP, CD31 and DAPI. These two 60 micron sections were then aligned and stacked on top of each other to generate the 120 micron Z-stack shown in 2A, 2B, and 2C.

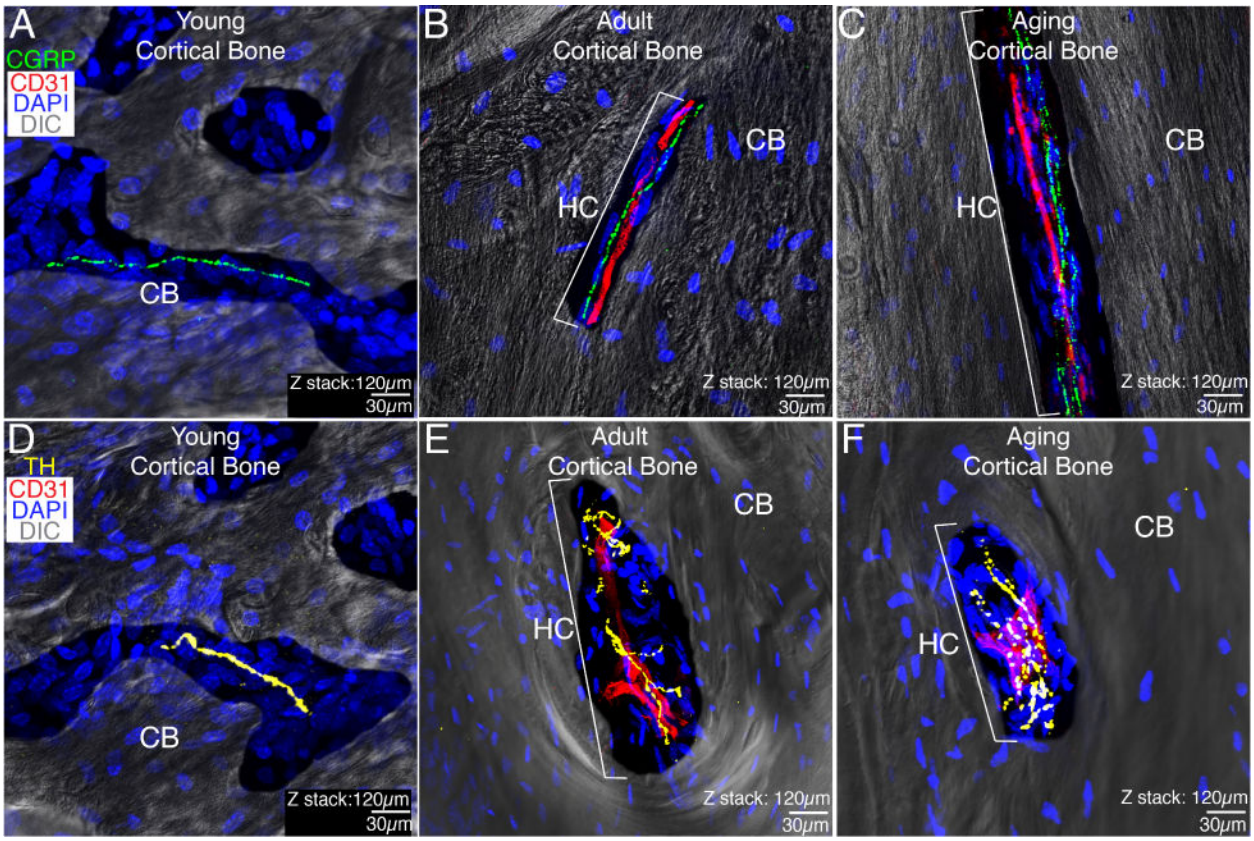

Figure 3. Blood vessels, sensory and sympathetic nerve fibers that innervate the cortical bone in the young, adult and aging femur

In these images, the cortical bone (CB) is imaged by differential interfere contrast (DIC) and nuclei within the cortical bone are stained by DAPI (blue). In the young animal, the CB is largely cartilaginous with some woven bone and there are not any well-formed Haversian canals (HC) or CD31+ blood vessels although occasional CGRP+ sensory fibers (A) and TH + sympathetic (D) nerve fibers can be observed. With aging, both the adult (B&E) and aging (C&F) cortical bone of the femur becomes mineralized and nearly all sensory or sympathetic nerve fibers in the adult and aging cortical bone are present in Haversian canals most of which are vascularized by CD31+ blood vessels. With age, the number of CD31+ Haversian canals declines, as does the percent of CD31+ Haversian canals that contain TH+ sympathetic nerve fibers. A similar decline was not observed in the percent of CD31+ Haversian canals innervated by CGRP+ sensory nerve fibers. It should be noted that we did not observe any sensory or sympathetic nerve fibers in the young, adult or aging subchondral bone. All confocal images are composed of 2 serially adjacent 60 micron sections = total z-stack of 120 microns.

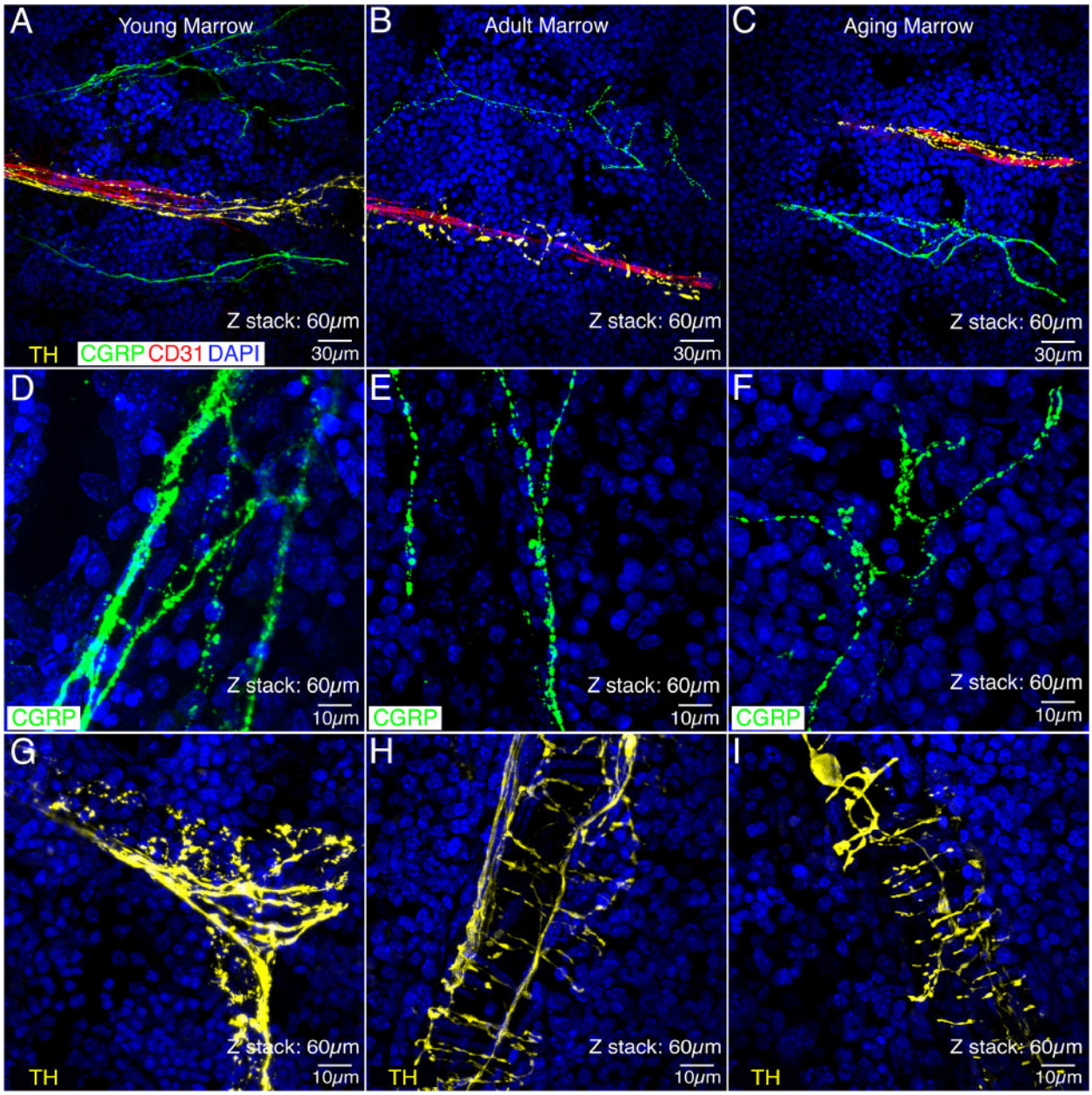

Figure 4. Sensory fibers, sympathetic fibers and blood vessels in the bone marrow of the young, adult and aging mouse femur

In these images, the sympathetic nerve fibers (yellow) are labeled by an antibody raised against tyrosine hydroxylase (TH), the sensory nerve fibers (green) are labeled with an antibody raised against calcitonin gene related peptide (CGRP) and the endothelial cells are labeled with an antibody raised against 140 kD glycoprotein know as platelet endothelial cell adhesion molecule which is also known as CD31 (red). Note that the TH+ sympathetic fibers in the bone marrow have a characteristic “corkscrew shaped” appearance (A, B, C, G, H, I) as they are tightly wrapped around blood vessels. In contrast, CGRP+ sensory nerve fibers have a much more linear appearance (D, E, F) and do not have the same intimate association with blood vessels (A, B, C). Also, note that there is not a significant decline in

either the density of the sensory or sympathetic nerve fibers innervation of the bone marrow with age, although sensory nerve fibers do appear to have more branch points with age and the intensity of TH immunoreactivity in the sympathetic fibers appears to decline with age (i.e. compare Figs. G vs. H or I). Confocal images in A, B and C were obtained from two serially adjacent tissue sections. The first 30 micron serial section was stained for TH, CD31, and DAPI. The second 30 micron serial section was stained for CGRP, CD31, and DAPI. These two 30 micron sections were then aligned and stacked on top of each other to generate the 60 micron Z-stack shown in A, B, and C. This figure shows the relationship of CGRP+ sensory, TH+ sympathetic, and CD31+ blood vessels in the young, adult and aging bone marrow, respectively. As one can see in all of these images, the TH+ sympathetic nerve fibers have a distinct morphology and closer relationship to CD31+ blood vessels as compared to the CGRP+ sensory nerve fibers. In (D, E, and F) single 60 micron sections were stained for CGRP and DAPI and in G, H, and I single 60 micron sections were stained with TH and DAPI.

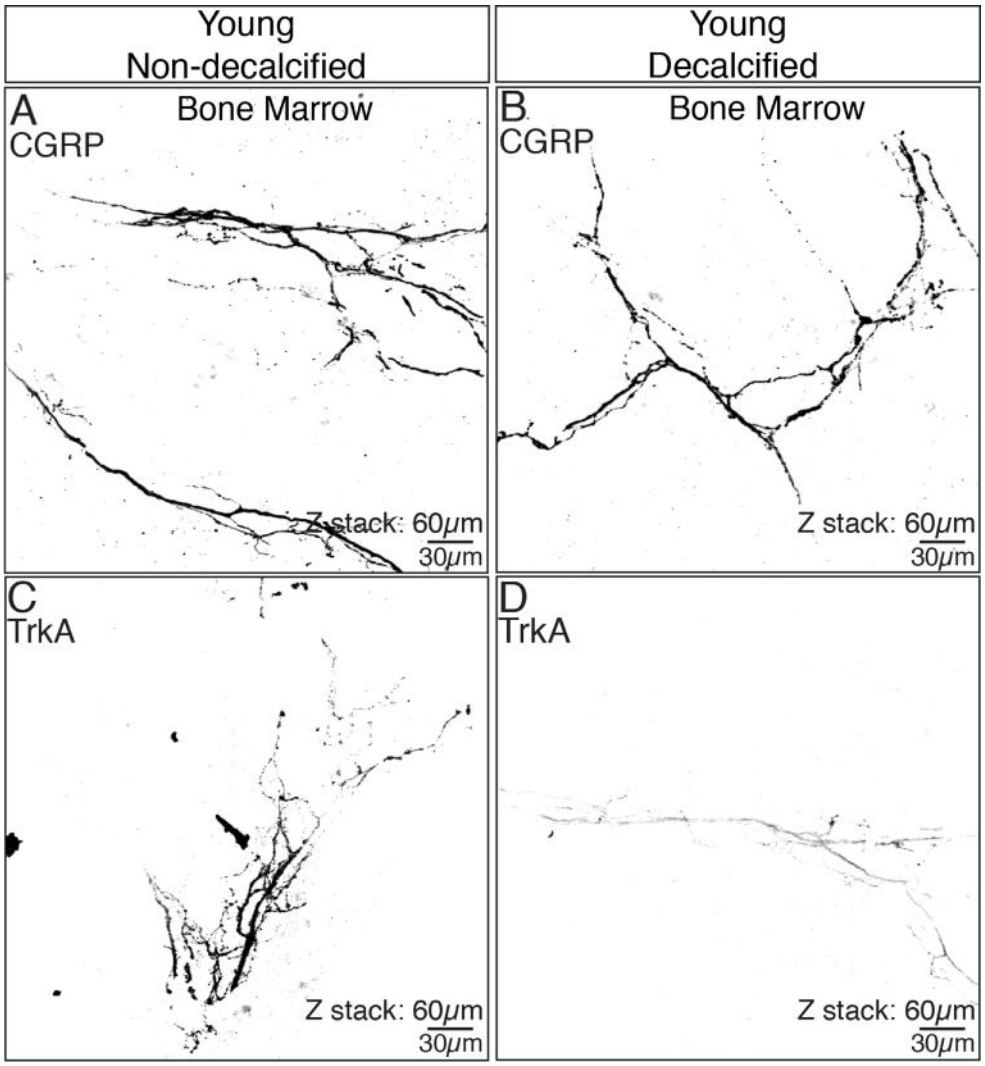

Figure 5. The process of decalcification significantly impacts the ability to detect TrkA but not CGRP immunoreactivity in bone

In the non-decalcified young femur, robust staining of both CGRP (A) and TrkA (C) are observed in the bone marrow. However, while robust CGRP immunoreactivity is still detected following decalcification of the young bone (B), TrkA immunoreactivity (D) markedly declines. These data show that the decalcification procedure (which is required to cut tissue sections from most calcified tissues) can have a marked and negative impact on some but not all antigens. These confocal images were obtained from a single 60 micron section of young bone.

Table 1

Table of primary antibodies used for immunological staining

Antigen	Immunogen	Manufacturer, species raised in, mono/polyclonal, catalogue and lot number	Dilution used	Reference
CGRP	Synthetic rat Tyr-CGRP conjugated to keyhole limpet hemocyanin (37 amino acids)	Sigma Chemical Co., rabbit, polyclonal, Cat# C8198, Lot# 059K4841	1 :10,000	(Gibson et al., 1984) (Kruger et al., 1989) (Peleshok and Riberio-da-Sila, 2011)
TH	Tyrosine hydroxylase from rat phenochromocytoma denatured with sodium dodecyl sulfate (complete sequence)	Millipore, rabbit, polyclonal, Cat#AB152, Lot# 2066692	1 :1000	(Wang et al., 1991) (Pelling et al., 2011)
CD31	129/Sv mouse-derived endothelioma cell line tEnd.1	BD Pharmingen, rat, polyclonal, Cat#550274	1 :500	(Baldwin et al., 1994) (Vecchi et al., 1994)
NGF	N-terminus of NGF mature chain of mouse origin	Santa Cruz, rabbit, polyclonal, Cat# SC-548, Lot# J1909	1 :1000	(Balzamino et al., 2014) (Perovic et al., 2012)
TrkA	Mouse myeloma cell line NSO-derived recombinant rat TrkA	R&D Systems, goat, polyclonal, Cat# AF1056, Lot# VFA011411	1 :1000	(Usoskin et al., 2015) (Evans et al., 2013)
p75	Recombinant mouse NGF Receptor p75 extracellular fragment	Millipore, rabbit, polyclonal, Cat# AB1554, Lot# 2502888	1 : 1000	(Neirinckx et al., 2015) (Datta-Mitra et al., 2015)

Table 2

The qualitative assessment of the impact that the decalcification process has on the ability to immunohistochemically detect neuronal and vascular antigens in the mouse femur

Note that several antigens are negatively affected by the decalcification process and of the 6 antigens presented here, only CGRP, TH, and CD31 showed little or no decline in immunoreactivity when comparing young non-decalcified vs. decalcified femur. These results suggest that using a positive control such as the young femur (which is largely cartilaginous and can be sectioned with or without decalcification) is essential when comparing young, adult and aging bone as the extent and length of the decalcification process may impact the ability to detect an antigen of interest.

	Non-decalcified Young Marrow	Decalcified Young Marrow	Decalcified Adult Marrow	Decalcified Aging Marrow
CGRP	+ + +	+ + +	+ + +	+ + +
TH	+ + +	+ + +	+ + +	+ + +
CD31	+ + +	+ + +	+ + +	+ + +
p75	+ + +	+	▬	▬
NGF	+ + +	+	▬	▬
TrkA	+ + +	+	+	+